

1 Synergistic remediation of aqueous Cd(II) by sewage sludge biochar via

2 P/Fe co-impregnation

3

4 Yunping Ji <sup>a,b,\*</sup>, Yarong Zhao <sup>c</sup>, Qingfeng Lv <sup>a</sup>, Fei Gao <sup>d</sup>

5 <sup>a</sup> School of Civil Engineering and Mechanics, Lanzhou University, Lanzhou 730000,  
6 China

7 <sup>b</sup> China Railway First Survey and Design Institute Group Co., Ltd., Lanzhou 730000,  
8 China

9 <sup>c</sup> Zhejiang Huancheng Environmental Protection Technology Co., Ltd., Hangzhou  
10 310012, China

11 <sup>d</sup> China Railway 21st Bureau Group Co., Ltd., Lanzhou 730070, China

12 \*Corresponding author: Yunping Ji (shaopei13698@163.com)

14 **Text S1** Calculation Formulas and Adsorption Models

15 The sorption amount ( $q_e$ , mg/g) were computed according to Eq. (S1).

16 
$$q_e = \frac{(C_0 - C_e) \times V}{m} \quad (\text{S1})$$

17 Where  $C_0$  and  $C_e$  are the initial and final concentration of Cd(II) (mg/L), respectively;  
18  $q_e$  is sorption amount (mg/g);  $V$  is the solution volume (mL); and  $m$  is the mass of  
19 adsorbent (mg).

20 Adsorption kinetics model: the pseudo-first-order model (Eq. S2), the pseudo-  
21 second-order model (Eq. S3), and intra-particle diffusion model (Eq. S4) were used  
22 for fitting analysis.

23 
$$\ln(q_e - q_t) = \ln q_e - k_1 t \quad (\text{S2})$$

24 
$$\frac{t}{q_t} = \frac{1}{q_e^2 k_2} + \frac{t}{q_e} \quad (\text{S3})$$

25 
$$q_t = K_{id} t^{1/2} + C_i \quad (\text{S4})$$

26 Where  $q_e$  and  $q_t$  are the sorption capacity at the equilibrium time and time " $t$ "  
27 time (mg/g), respectively;  $k_1$  and  $k_2$  represent sorption rate constant of the pseudo-  
28 first-order (1/min) and the pseudo-second-order (g/mg·min), respectively;  $K_{id}$   
29 (mg/g·min<sup>1/2</sup>) is rate constants of intra-particle diffusion, respectively;  $C_i$  is constant  
30 of the intra-particle diffusion model.

31 Adsorption isotherm model: the Langmuir model (Eq. S5), Freundlich model (Eq.  
32 S6), and Temkin model (Eq. S7) were used to fit these data.

33 
$$\frac{C_e}{q_e} = \frac{1}{q_{\max} K_L} + \frac{C_e}{q_{\max}} \quad RL = \frac{1}{1 + C_0 K_L} \quad (\text{S5})$$

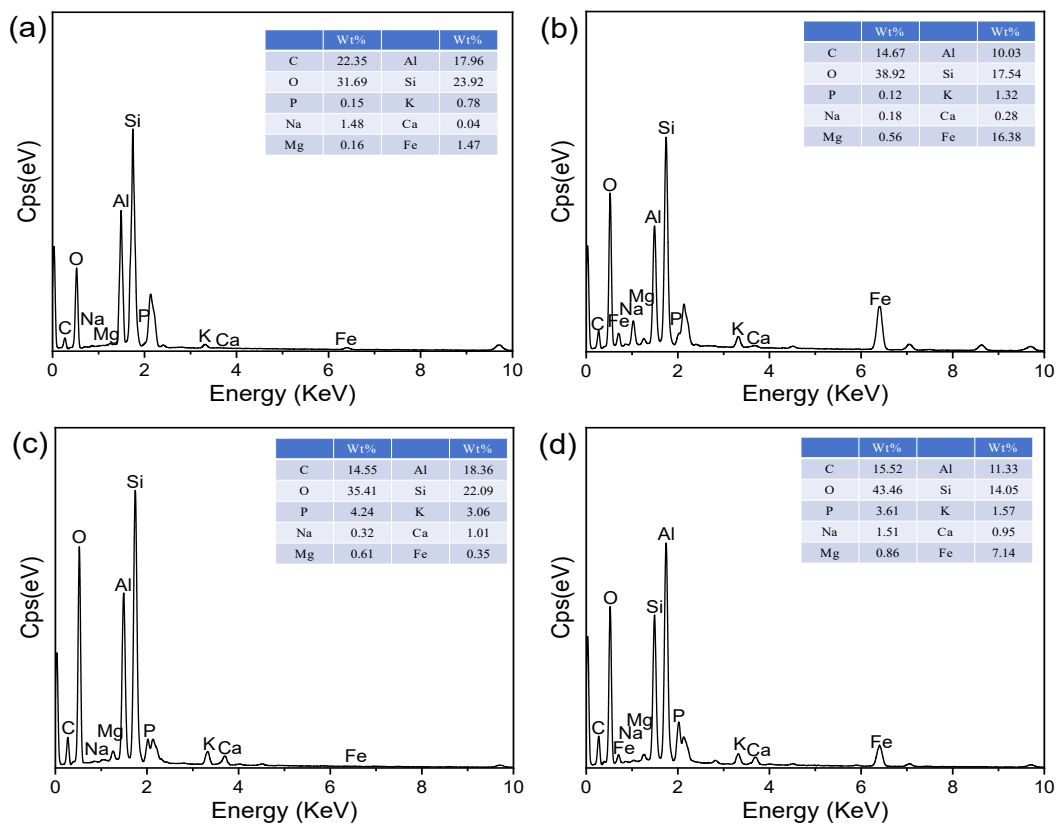
34 
$$\ln q_e = \ln K_F + \frac{1}{n} \ln C_e \quad (\text{S6})$$

35 
$$q_e = B_T \ln A_T + B_T \ln C_e \quad (\text{S7})$$

36 Where  $q_e$  is the sorption capacity at equilibrium (mg/g);  $C_e$  is the concentration  
37 of Cd(II) at sorption equilibrium (mg/L);  $q_{\max}$ , and  $K_L$  are the maximum sorption  
38 capacity of Cd(II) (mg/g), and Langmuir equilibrium constant (L/mg), respectively;  $K_F$   
39 and  $n$  represent the Freundlich affinity coefficient (mg<sup>1-n</sup>·L<sup>n</sup>/g) and Freundlich  
40 constant related to the surface site heterogeneity, respectively;  $A_T$  (1/g) and  $B_T$  (kJ/mol)  
41 are Temkin constants.

42 **Text S2** Characterization analysis

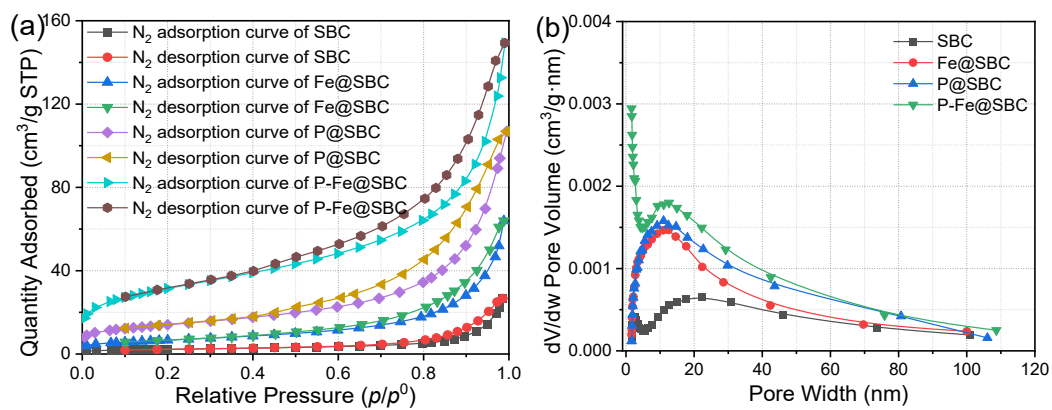
43 The N<sub>2</sub> adsorption-desorption isotherms were measured at 77 K using an  
44 automatic surface area and porosity analyzer (ASAP 2020 Plus HD88, Micromeritics,  
45 USA). Prior to analysis, all samples were degassed under vacuum at 150 °C for 6 h to  
46 remove moisture and impurities. The specific surface area (SSA) was calculated using  
47 the Brunauer-Emmett-Teller (BET) equation, while the pore size distribution and total  
48 pore volume were determined from the desorption branch of the isotherms using the  
49 Barrett-Joyner-Halenda (BJH) model. The microstructure of the biochars was tested  
50 by scanning electron microscopy (SEM-EDS, JSM-7500F, JEOL, Japan). The surface  
51 functional groups were analysed by Fourier transform infrared spectroscopy (FTIR,  
52 Nicolet-460, Thermo Fisher, USA). Crystalline forms in biochars were investigated  
53 using an X-ray diffraction analyser (XRD, D8, Bruker, Germany). The elemental of  
54 the biochars was analyzed by X-ray photoelectron spectroscopy (XPS, Escalab 250 xi,  
55 Thermo Fisher, USA). The degree of graphitization and disordered structural  
56 characteristics were revealed by Raman spectroscopy (Thermo Fisher, USA).



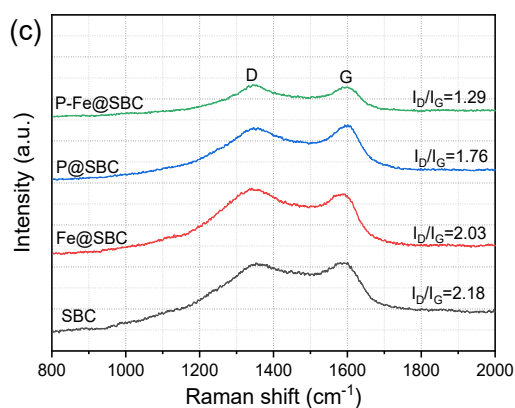
57

58

59 Fig. S1 EDS analysis of different adsorbents (a: SBC, b: Fe@SBC, c: P@SBC and d:  
60 P-Fe@SBC ).

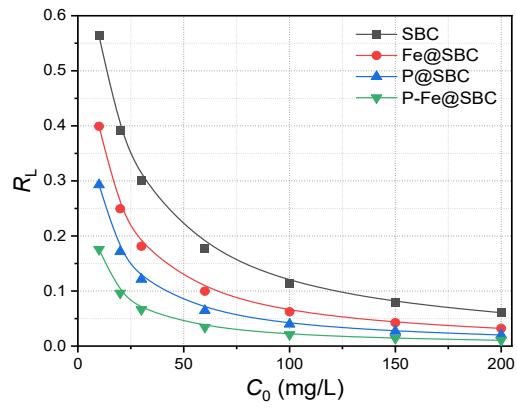


61



62

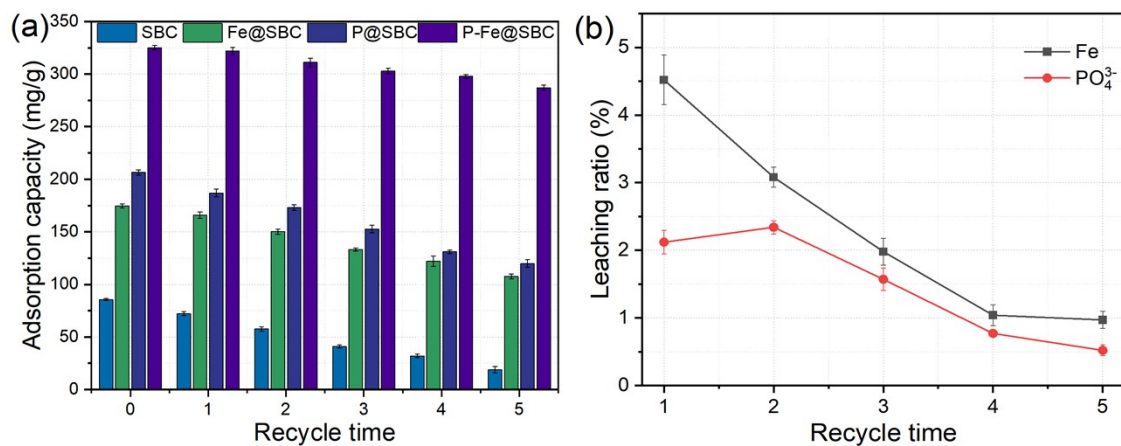
63 Fig. S2 N<sub>2</sub> adsorption-desorption isotherms (a), pore size distribution curves (b),  
 64 Raman analysis (c) of different adsorbents.



65

66 **Fig. S3** Separation factors ( $R_L$ ) of different adsorbents for Cd(II) removal

67



68

69 **Fig. S4** Reusability of the adsorbents for Cd(II) removal over five adsorption-  
 70 desorption cycles (a). Release concentration of Fe and phosphate after adsorption by  
 71 different regenerated P-Fe@SBC (b).

72 Table S1 Comparison of the maximum adsorption capacity of different adsorbents for Cd<sup>2+</sup>.

Adsorbent	Maximum adsorption capacity	References
Iron and silicon modified biochar	31.66	1
Chitosan@coconut shell-derived biochar	63.88	2
HCl-modified biochar	68.22	3
EDTA functionalized Mg/Al hydroxides modified biochar	204.53	4
Cysteine-grafted magnesium-modified biochar	223.7	5
Hydroxyl-functionalized Fe/Ni-biochar	229.52	6
Multifunctional magnetic biochar	292	7
P-Fe@SBC	326	This work

73

74

75 1. H. Wu, L. N. Liu, Y. G. Zhuo, R. M. Ellam, K. S. Yan, J. C. Liu and J. C. Tang, *Bioresour. Technol.*, 2024, **401**, 130745.

77 2. G. H. Mo, J. Xiao and X. Gao, *Biomass Convers. Bior.*, 2022, **13**, 16737–16752.

78 3. J. W. Wu, T. Wang, Y. S. Zhang and W. P. Pan, *Bioresour. Technol.*, 2019, **291**, 121859.

79 4. Y. F. Wang, J. E. Li, L. Xu, D. Wu, Q. N. Li, Y. H. Ai, W. Liu, D. N. Li, Y. T. Zhou, B. Y. Zhang, N. Guo, Y. Tao and Y. Zhang, *Separation and Purification Technology*, 2024, **335**, 126199.

82 5. A. Y. Li, C. H. Ye, Y. H. Jiang and H. Deng, *Bioresour. Technol.*, 2023, **386**, 129515.

83 6. H. Wang, Q. Chen, H. X. Xia, R. R. Liu and Y. H. Zhang, *Separation and Purification Technology*, 2024, **328**, 125074.

85 7. G. H. Mo, F. P. Li, J. N. Xiao, Z. G. Han and Z. M. Zhang, *Chemical Engineering Journal*, 2025, **526**, 171319.

87